

Analytical solution to seepage problem from a soil channel with a curvilinear bottom

Bhagu R. Chahar

Department of Civil Engineering, Indian Institute of Technology Delhi, New Delhi, India

Received 25 March 2005; revised 28 September 2005; accepted 13 October 2005; published 14 January 2006.

[1] An exact analytical solution for the quantity of seepage from a semicircular channel is not available because of difficulties in the conformal mapping. In the present study an inverse method has been used to obtain an exact solution for seepage from a curved channel whose boundary maps along a circle onto the hodograph plane. The solution involves inverse hodograph and Schwarz-Christoffel transformation. The solution also includes a set of parametric equations for the shape of the channel perimeter and loci of phreatic lines. The channel shape is an approximate semiellipse with the top width as the major axis and twice the water depth as the minor axis and vice versa. The average of the corresponding ellipse and parabola gives nearly the exact shape of the channel. Also, this channel is non-self-intersecting and is feasible from a very deep channel to a very wide channel, unlike Kozeny's trochoid shape, which is self-intersecting for a top width to depth ratio less than 1.14. Its seepage function is a linear combination of seepage functions for a slit and a strip. However, this channel allows more seepage loss than a trochoid channel. A special case of the resulting channel is an approximate semicircular section.

Citation: Chahar, B. R. (2006), Analytical solution to seepage problem from a soil channel with a curvilinear bottom, *Water Resour. Res.*, 42, W01403, doi:10.1029/2005WR004140.

1. Introduction

[2] Study of seepage from curved channels is important because of its applications in areas of irrigation engineering, hydrology, reservoir management, and groundwater recharge. A semicircular channel is the most hydraulically efficient section and hence is also the most economical section as it has the least cross-sectional area and wetted perimeter [Chow, 1973]. J. Kozeny [Harr, 1962; Polubarinova-Kochina, 1962; Muskat, 1982] investigated seepage from a curved channel using Zhukovsky's function and found that the resultant channel has trochoid shape. Anakhaev [2004] obtained a solution for curvilinear watercourses by representing the watercourse profiles in the Zhukovsky plane by means of the equation of a family of lemniscates and by using the conformal mapping and showed that a special case reduces to Kozeny's trochoid shape. Hunt [1972] presented an approximate solution for seepage from a shallow channel of an arbitrary cross section. N. N. Verigin [Kovacs, 1981; Aravin and Numerov, 1965] analytically found an approximate solution for a circular section in terms of a rapidly converging series. Kacimov [2003] pointed out the mistake in Verigin's solution. Ilyinskii and Kacimov [1984] found the optimal shape of a curved irrigation channel from the point of view of minimum seepage loss using the inverse boundary value problem method. Furthermore, Kacimov and Obnosov [2002] used the inverse method along with hodograph and conformal mapping to find the shape of a soil channel of constant hydraulic gradient. Swamee and Kashyap [2001] obtained seepage from nonpolygon canals, including

circular canals using the finite difference method; however, there are some drawbacks in their solution, as highlighted by Kacimov [2003]. Approximate solutions to find the quantity of seepage from canals by numerical (finite difference, finite element, boundary integral, etc.) methods [Remson et al., 1971; Huyakorn and Pinder, 1983; Liggett and Liu, 1983] have gained importance because of easy availability of high-speed digital computers along with specialized software. These methods can be used to quantify the seepage from curved channels. However, numerical methods result only in a numerical value as a problem-specific solution. Therefore generalized solutions in the functional form are not possible through numerical methods. An exact analytical solution for a semicircular channel is not achievable since its geometry maps in curvilinear shapes onto hodograph and inverse hodograph planes, for which Schwarz-Christoffel transformation is impossible. One possible way out is an inverse method where the shape of the unknown channel is searched as part of a solution [Ilyinskii and Kacimov, 1984; Kacimov and Obnosov, 2002]. Using the inverse method, an exact solution for seepage from a curved channel whose boundary maps along a circle onto the hodograph plane is presented. A special case of the resulting channel has been compared with a semicircular shape.

2. Analytical Solution

[3] The pattern of seepage from a curvilinear-bottomed symmetrical channel of top width T (m) and water depth y (m) in a homogeneous and isotropic porous medium of infinite extent is shown in Figure 1a. The effects of capillarity, infiltration, and evaporation are ignored. It is also assumed that the flow is steady and satisfies Darcy's

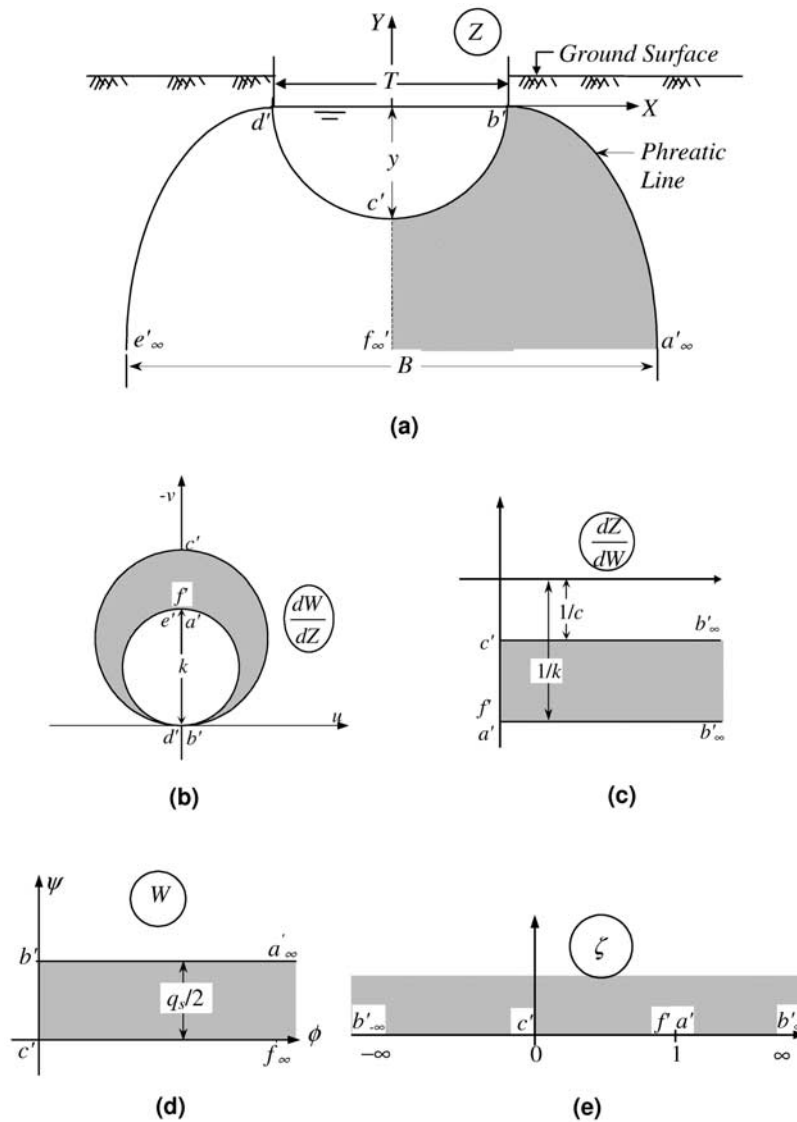


Figure 1. Seepage from a curvilinear-bottomed channel. (a) Physical plane, (b) hodograph plane, (c) inverse hodograph plane, (d) complex potential plane, and (e) auxiliary plane.

law. In view of the significant length of the channel the seepage flow can be considered two-dimensional in the vertical plane. Because of vertical symmetry the solution for the half domain ($a'b'c'f'a'$) is sought. The complex potential is defined as $W = \phi + i\psi$, where ϕ is the velocity potential (m^2/s), which is equal to hydraulic conductivity k (m/s) times the head h (m), and ψ is the stream function (m^2/s), which is constant along streamlines. If the physical plane is defined as $Z = X + iY$, then Darcy's law yields $u = \partial\phi/\partial X = -k(\partial h/\partial X)$ and $v = \partial\phi/\partial Y = -k(\partial h/\partial Y)$, where u and v are velocity or specific discharge vectors in X and Y directions, respectively. In the velocity hodograph plane ($dW/dZ = u - iv$) the phreatic line $a'b'$ will map along a circle of radius k with the center at $(0, k/2)$. Since a' lies at a very large depth, the hydraulic gradient is unity, and the seepage velocity becomes k in the vertically downward direction. The channel boundary $b'c'd'$ is an equipotential line, so the seepage velocity is normal to the boundary, and in the hodograph plane it will map a curvilinear path. However, the exact

shape of the curve is not known. It is assumed that the channel boundary maps along a circle of diameter c in the hodograph plane.

[4] The inverse hodograph dZ/dW (Figure 1c) and the complex potential W (Figure 1d) for half of the physical flow domain have been drawn following the standard steps [Strack, 1989; Strack and Asgian, 1978]. The dZ/dW plane and W plane have been mapped onto the upper half of an auxiliary ($\text{Im } \zeta > 0$) plane (Figure 1e) using the Schwarz-Christoffel conformal transformation [Harr, 1962; Polubarinova-Kochina, 1962].

[5] Mapping the W plane onto the ζ plane results in (for details of the mapping steps, refer to Appendix A or Chahar [2005])

$$W = \frac{q_s}{2\pi} \int_0^\zeta \frac{dt}{(t-1)\sqrt{t}} = \frac{q_s}{2\pi} \ln \left| \frac{\sqrt{\zeta} - 1}{\sqrt{\zeta} + 1} \right|, \quad (1)$$

where q_s is the quantity of seepage loss from unit length of channel (m^2/s) and t is a dummy variable. Taking the derivative of equation (1),

$$\frac{dW}{d\zeta} = \frac{q_s}{2\pi(1-\zeta)\sqrt{\zeta}}. \quad (2)$$

Similarly, mapping the dZ/dW plane onto the ζ plane results in

$$\frac{dZ}{dW} = \frac{1}{\pi} \left(\frac{1}{k} - \frac{1}{c} \right) \int_0^{\zeta} \frac{dt}{\sqrt{t(t-1)}} - \frac{i}{c}. \quad (3)$$

Equation (3) acquires a different form (see Appendix A) in the different regions $c'f'a'$ ($0 \leq \zeta \leq 1$), $d'b'$ ($1 \leq \zeta < \infty$), and $c'b'$ ($-\infty < \zeta \leq 0$). Multiplying equations (2) and (3) and then integrating yields

$$Z = \frac{q_s}{2\pi^2} \left(\frac{1}{k} - \frac{1}{c} \right) \int_0^{\zeta} \left(\int_0^t \frac{d\tau}{\sqrt{\tau(\tau-1)}} \right) \frac{dt}{(1-t)\sqrt{t}} - \frac{iq_s}{2\pi c} \int_0^{\zeta} \frac{dt}{(1-t)\sqrt{t}} - iy, \quad (4)$$

where τ is a dummy variable. Along the channel perimeter $c'b'$ ($-\infty < \zeta \leq 0$),

$$Z = \frac{q_s}{\pi c} \tan^{-1} \sqrt{-\zeta} - i \left(y - \frac{2q_s}{\pi^2} \left(\frac{1}{k} - \frac{1}{c} \right) \int_0^{\sinh^{-1} \sqrt{-\zeta}} \frac{\tau d\tau}{\cosh \tau} \right). \quad (5)$$

Separating real and imaginary parts at point b' ($\zeta = -\infty$; $Z = T/2$),

$$T = \frac{q_s}{c} \quad (6)$$

$$y = \frac{2q_s}{\pi^2} \left(\frac{1}{k} - \frac{1}{c} \right) 2G, \quad (7)$$

where $G = 0.915965594\dots =$ Catalan's constant. Combining equations (5), (6), and (7),

$$\frac{Y}{y} = \frac{1}{2G} \left(\int_0^{\sinh^{-1} \tan(\pi X/T)} \frac{\tau d\tau}{\cosh \tau} - 2G \right), \quad (8)$$

which defines the shape of the channel perimeter in Cartesian coordinates. Furthermore, combining equations (4), (6), and (7) in the phreatic line region $d'b'$ ($1 \leq \zeta < \infty$),

$$Z = \frac{T}{2} + \frac{y}{2G} \int_{\cosh^{-1} \sqrt{\zeta}}^{\infty} \frac{\tau d\tau}{\sinh \tau} + i \left(T + \frac{\pi^2 y}{4G} \right) \ln \tanh \left(\frac{\cosh^{-1} \sqrt{\zeta}}{2} \right). \quad (9)$$

Therefore the parametric equations for the phreatic line are

$$X = \frac{T}{2} + \frac{y}{2G} \int_{\cosh^{-1} \sqrt{\zeta}}^{\infty} \frac{\tau d\tau}{\sinh \tau} \quad (10a)$$

$$Y = \left(T + \frac{\pi^2 y}{4G} \right) \ln \tanh \left(\frac{\cosh^{-1} \sqrt{\zeta}}{2} \right). \quad (10b)$$

The integrals in equations (8) and (10a) involving hyperbolic cosine and sine functions can be expressed as infinite series expansions (Appendix A) or evaluated numerically. The phreatic line has a vertical asymptote at $Y = -i\infty$, i.e., at the point a' ($\zeta = 1$), given by

$$X = \frac{T}{2} + \frac{\pi^2 y}{8G}. \quad (11)$$

Hence the width of seepage flow at infinite depth B (m) comes out

$$B = 2X_{\infty} = T + \frac{\pi^2 y}{4G}. \quad (12)$$

[6] The distribution of the velocity of seeping water normal to the channel perimeter can be found by using equation (3) along $c'b'$ ($-\infty < \zeta \leq 0$) as

$$\frac{dZ}{dW} = \frac{1}{u-iv} = \frac{2}{\pi} \left(\frac{1}{k} - \frac{1}{c} \right) \sinh^{-1} \sqrt{-\zeta} - \frac{i}{c}. \quad (13)$$

Substituting the values of c and ζ and then manipulating,

$$V = \frac{k(T/y + \pi^2/4G)}{\sqrt{((\pi \sinh^{-1} \tan(\pi X/T))/2G)^2 + (T/y)^2}}. \quad (14)$$

2.1. Quantity of Seepage

[7] The steady seepage loss from a channel in the hydrogeological conditions of Figure 1a can be expressed as

$$q_s = k(T + Ay) = kB = kyF_s, \quad (15)$$

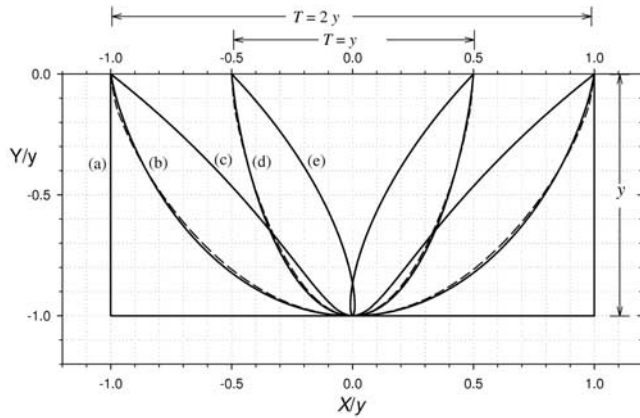


Figure 2. Comparison of seepage loss with other channel shapes. Rectangular channel with $T/y = 2$ (labeled a), curvilinear-bottomed channel (solid curve) and average of parabolic and elliptical shape (dashed curve) for $T/y = 2$ (labeled b), trochoid channel with $T/y = 2$ (labeled c), curvilinear-bottomed channel (solid curve) and average of parabolic and elliptical shape (dashed curve) for $T/y = 1$ (labeled d), and self-intersecting Trochoid at $T/y = 1$ (labeled e).

where A is Vedernikov's parameter [Harr, 1962] and F_s is the seepage function [Chahar, 2000; Swamee et al., 2000, 2001b], which is a dimensionless function of channel geometry and boundary condition. Using the value of c from equation (6) in equation (7),

$$q_s = k \left(\frac{\pi^2}{4G} y + T \right) = ky \left(\frac{\pi^2}{4G} + \frac{T}{y} \right). \quad (16)$$

Therefore Vedernikov's parameter and seepage function for this channel are

$$A = \frac{\pi^2}{4G} \approx \pi(4 - \pi) \approx 2.69676 \quad (17a)$$

$$F_s = \frac{\pi^2}{4G} + \frac{T}{y}, \quad (17b)$$

respectively. It is interesting to note that the Vedernikov's parameter is identical to that of a slit [Chahar, 2001]. Furthermore, equations (6) and (7) at $c = 2k$ yield

$$q_s = 2kT = \frac{\pi^2}{2G} ky. \quad (17c)$$

Therefore

$$\frac{T}{y} = \frac{\pi^2}{4G}. \quad (17d)$$

The quantity of seepage given by equation (17c) is the minimum for a fixed area of the channel [Chahar, 2005]. Thus the top width to depth ratio equal to $\pi^2/4G$ results in a minimum seepage loss channel section. Ilyinskii and Kacimov [1984] also got a result identical to equation (17c) for their q_s optimal channel. Therefore a particular case ($c = 2k$) of the present channel is the optimal channel studied by Ilyinskii and Kacimov [1984]. Furthermore, equation (16) gives $q_s = ky\pi^2/4G$ for a slit (a very narrow and deep channel, i.e., $T/y \rightarrow 0$) and $q_s = kT$ for a strip (a very wide and shallow channel, i.e., $T/y \rightarrow \infty$). Comparison of seepage loss from an optimal section given by equation (17c) with those from slit and strip sections shows (1) that the seepage loss from the minimum seepage loss section is twice that from the same top width strip section or the same depth slit section and (2) that for the same quantity of seepage the top width of a strip section is twice the top width of the corresponding minimum seepage loss section or the water depth in a slit section is twice that of the corresponding minimum seepage loss section. This halving feature of optimal sections, as compared with geometrically degenerated shapes (slit and strip), was also confirmed by Kacimov [2001, and references therein] for channels, drains, electrical condensers, and dams.

[8] As per the comparison theorem [Kacimov, 2003] the value of q_s for any arbitrary channel is bounded from below and above by the following inequality:

$$q_i < q_s < q_c, \quad (18)$$

where q_i and q_c are seepage discharges from an arbitrary inscribed channel and an arbitrary comprising channel, respectively. A rectangular channel is selected as a comprising channel, and a Kozeny's trochoid channel is selected as an inscribed channel (see Figure 2). The shape of the present channel perimeter involving a hyperbolic cosine integral is evaluated through numerical integration using MATLAB. All three channels have the same y and T but differ in their shape such that a monotonic deformation from one shape to another gives a monotonic increase of the seepage losses according to equation (18). The shape of the Kozeny's trochoid can be given by the following parametric equations [Muskat, 1982]:

$$Y = y \cos(\pi\psi/q_i) \quad (19a)$$

$$X + \psi/k = y \sin(\pi\psi/q_i), \quad (19b)$$

where the quantity of seepage q_i is given by

$$q_i = ky(2 + T/y), \quad (19c)$$

so the Vedernikov's parameter for the trochoid channel is equal to 2. The main limitation of a trochoid channel is that it cannot be too deep. From equations (19a) and (19b),

$$\frac{dY}{dX} = \frac{\sin(\pi\psi/q_i)}{\cos(\pi\psi/q_i) - q_i/\pi ky} = \frac{\sqrt{y^2 - Y^2}}{Y - q_i/\pi k}. \quad (20)$$

Table 1. Characteristics of the Present Curvilinear-Bottomed Channel

Approximate Semicircular ($T/y = 2$)				General Case ($T/y = 3$)				
$\pm X/y$	Approximate Radius	Percent Error	V/k	Y/y				
				$\pm X/y$	Present Channel	Parabolic Shape	Elliptical Shape	Average of (7) and (8)
0.00	1.0000	0.0000	2.3469	0.00	-1.0000	-1.0000	-1.0000	-1.0000
0.06	0.9994	-0.0623	2.3392	0.09	-0.9976	-0.9964	-0.9982	-0.9973
0.10	0.9983	-0.1727	2.3257	0.15	-0.9933	-0.9900	-0.9950	-0.9925
0.16	0.9956	-0.4391	2.2931	0.24	-0.9827	-0.9744	-0.9871	-0.9808
0.20	0.9932	-0.6817	2.2635	0.30	-0.9728	-0.9600	-0.9798	-0.9699
0.26	0.9886	-1.1374	2.2079	0.39	-0.9538	-0.9324	-0.9656	-0.9490
0.30	0.9850	-1.4979	2.1639	0.45	-0.9382	-0.9100	-0.9539	-0.9320
0.36	0.9789	-2.1134	2.0881	0.54	-0.9103	-0.8704	-0.9330	-0.9017
0.40	0.9743	-2.5659	2.0317	0.60	-0.8884	-0.8400	-0.9165	-0.8783
0.46	0.9671	-3.2905	1.9391	0.69	-0.8507	-0.7884	-0.8879	-0.8382
0.50	0.9621	-3.7915	1.8723	0.75	-0.8220	-0.7500	-0.8660	-0.8080
0.56	0.9546	-4.5417	1.7654	0.84	-0.7731	-0.6864	-0.8285	-0.7574
0.60	0.9498	-5.0198	1.6897	0.90	-0.7363	-0.6400	-0.8000	-0.7200
0.66	0.9434	-5.6571	1.5697	0.99	-0.6741	-0.5644	-0.7513	-0.6578
0.70	0.9401	-5.9929	1.4853	1.05	-0.6275	-0.5100	-0.7141	-0.6121
0.76	0.9372	-6.2819	1.3509	1.14	-0.5484	-0.4224	-0.6499	-0.5362
0.80	0.9373	-6.2673	1.2551	1.20	-0.4884	-0.3600	-0.6000	-0.4800
0.86	0.9422	-5.7796	1.0978	1.29	-0.3849	-0.2604	-0.5103	-0.3853
0.90	0.9499	-5.0097	0.9786	1.35	-0.3038	-0.1900	-0.4359	-0.3129
0.96	0.9721	-2.7887	0.7496	1.44	-0.1530	-0.0784	-0.2800	-0.1792
1.00	1.0000	0.0000	0.0719	1.50	0.0000	0.0000	0.0000	0.0000

At the central point, $Y = y$, so $dY/dX = 0$ except when the denominator is zero. In that case, dY/dX is indeterminate, and the trochoid becomes self-intersecting and loses its usefulness. At this limiting case,

$$y = \frac{q_i}{\pi k} = \frac{T + 2y}{\pi} \Rightarrow T = (\pi - 2)y. \tag{21}$$

For a practical application of a trochoid shape, T/y must be greater than $\pi - 2$. So there is a typo in *Kacimov's* [2003] note for this inequality. Similarly, the channel of constant hydraulic gradient investigated by *Kacimov and Obnosov* [2002] becomes self-intersecting at larger depths ($c \geq 0.5k$). Figure 2 also compares the investigated curved channel and a self-intersecting case of a trochoid for $T/y = 1$. The present curved channel does not have such a limitation at any y and T .

[9] Making use of *Morel-Seytoux's* [1964] exact solution for the seepage from a rectangular channel, *Chahar* [2000] and *Swamee et al.* [2000] obtained closely approximate explicit expression for the seepage function, while *Chahar* [2001] presented the solution for *Vedernikov's* parameter in graphical form. Using these results, it can be verified that the following inequality is always true for any set of y and T :

$$2 + \frac{T}{y} < \frac{\pi^2}{4G} + \frac{T}{y} < \left((\pi^2/4G)^{0.77} + (T/y)^{0.77} \right)^{1.3}. \tag{22}$$

2.2. Salient Features

[10] The curved channel described by equation (8) possesses many interesting properties. It approximately represents a semiellipse with major and minor axes equal to T and $2y$, respectively, and vice versa. Actually, it always lies between the semiellipse and a parabola (inscribed in a rectangle with sides T and y), and any of its coordinates is

almost exactly the average of the coordinates of the corresponding ellipse and parabola (see Figure 2 for $T/y = 2$ and $T/y = 1$, and see Table 1 for $T/y = 3$). This channel is non-self-intersecting and hence is feasible from $T/y \rightarrow 0$ (slit) to $T/y \rightarrow \infty$ (strip). In fact this is the basic shape of the channel, and it highlights the importance of expressing seepage loss in terms of seepage function. It can be noted from equation (17b) that the seepage function is a linear combination of seepage functions for a slit ($\pi^2/4G$) and a strip (T/y), respectively [*Chahar, 2000; Swamee et al., 2001a*]. On the other hand, the seepage functions for other channels are power combination of $\pi^2/4G$ and T/y . For example, the power is 1.3 for an inscribing triangular channel and 0.77 for a comprising rectangular channel [*Chahar, 2000; Swamee et al., 2000*], whereas it is in between these limits for other feasible channels for same T/y .

[11] A semicircle is a special case of a semiellipse, and consequently, by adopting $T/y = 2$ the curved channel can be approximated into a semicircular channel. Figure 3 shows a comparison with a semicircular channel. Both the channels closely match each other; the maximum error is 6.3% (Table 1). Taking $T/y = 2$ in equation (14),

$$\frac{V}{k} = \frac{(1 + \pi^2/8G)}{\sqrt{((\pi \sinh^{-1} \tan(\pi X/T))/4G)^2 + 1}}. \tag{23}$$

This variation in the velocity of seeping water normal to the channel perimeter is plotted in Figure 3. The maximum velocity at the deepest point ($X/T = 0$) of the channel perimeter is

$$\frac{V}{k} = 1 + \frac{\pi^2}{8G} = 2.3469. \tag{24}$$

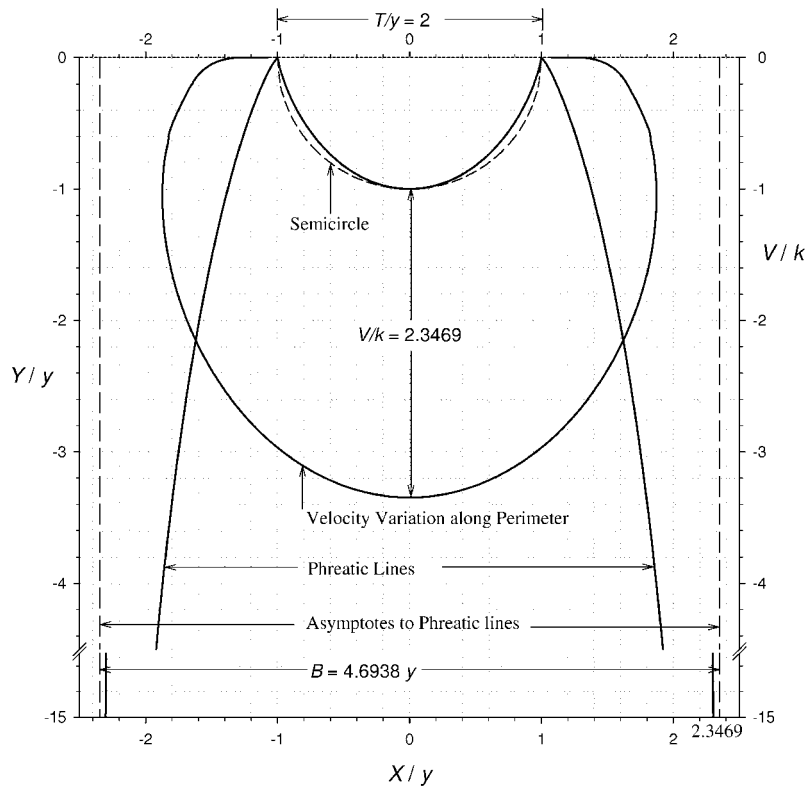


Figure 3. Variation in seepage velocity and location of phreatic line for an approximate semicircular channel (curvilinear-bottomed channel with $T/y = 2$).

Figure 3 also plots the phreatic lines by using $T/y = 2$ in equations (10a) and (10b). For an approximate semicircular channel the vertical asymptote of the phreatic line, the width of the flow at infinity, and the quantity of seepage reduce to

$$\frac{X}{y} = \frac{T}{2y} + \frac{\pi^2}{8G} = 2.3469, \tag{25a}$$

$$B = y \left(\frac{T}{y} + \frac{\pi^2}{4G} \right) = 4.6938y, \tag{25b}$$

$$q_s = 4.6938ky, \tag{25c}$$

respectively.

3. Conclusions

[12] An exact analytical solution for the quantity of seepage from a curved channel whose boundary maps along a circle onto the hodograph plane can be obtained using an inverse method along with inverse hodograph and Schwarz-Christoffel transformation. The shape of the channel is an approximate semiellipse. Nearly the exact shape of the channel can be obtained by averaging the corresponding ellipse and parabola. Unlike Kozeny’s trochoid shape and the constant gradient channel of Kacimov and Obnosov this channel is non-self-intersecting at greater depths and hence is feasible from a very narrow and deep channel (slit) to a very wide and shallow channel (strip). Indeed, this is the basic shape of the channel, and its seepage function is a linear combination of seepage functions for a slit and a strip. Also, Vedernikov’s parameter for the present channel is the

same as that for a slit. Moreover, the quantity of seepage from this channel is always greater than a feasible trochoid channel of the same top width to depth ratio. A particular case of this curved channel is close to a semicircular section.

Appendix A: Details of the Mapping Steps

A1. Mapping of a Complex Potential Plane

[13] Mapping the W plane onto the ζ plane results in

$$W = C_1 \int_0^\zeta \frac{dt}{(t-1)\sqrt{t}} + C_2, \tag{A1}$$

where C_1 and C_2 are constants. The branch of \sqrt{t} is selected which is positive at $t > 0$. The constants can be found by using values of W and ζ at two points in the W plane and the ζ plane. Using the values at point c' ($\zeta = 0, W = 0$) in equation (A1),

$$C_2 = 0 \tag{A2a}$$

at point b' ($\zeta = -\infty, W = iq_s/2$), so

$$\begin{aligned} \frac{iq_s}{2} &= C_1 \int_0^{-\infty} \frac{dt}{(t-1)\sqrt{t}} = C_1 \int_0^{-\infty} \frac{-idt}{(1-t)\sqrt{-t}} \\ &= iC_1 \int_0^{\infty} \frac{d\tau}{(1+\tau)\sqrt{\tau}} = iC_1\pi, \end{aligned} \tag{A2b}$$

and hence

$$C_1 = q_s/2\pi. \tag{A2c}$$

Substitution of C_1 and C_2 leads to equation (1). Along the center line $c'f'$ ($0 \leq \zeta \leq 1$) the mapping of equation (1) modifies to

$$W = -\frac{q_s}{2\pi} \ln\left(\frac{1-\sqrt{\zeta}}{1+\sqrt{\zeta}}\right). \tag{A3a}$$

In an infinite porous medium both points f' and a' are at infinity in the Z plane as well as in the W plane, and they map at $\zeta = 1$ in the ζ plane. When the point $\zeta = 1$ is crossed (i.e., a' is approached from f') in the ζ plane, there is a jump of $q_s/2$ in the W plane mapping. So the mapping for $d'b'$ ($1 \leq \zeta < \infty$) becomes

$$\begin{aligned} W &= \frac{q_s}{2\pi} \int_0^1 \frac{dt}{(1-t)\sqrt{t}} + \frac{iq_s}{2} + \frac{q_s}{2\pi} \int_1^\zeta \frac{dt}{(t-1)\sqrt{t}} \\ &= \frac{q_s}{\pi} \left(\frac{i\pi}{2} - \ln \tan\left(\frac{\sec^{-1} \sqrt{\zeta}}{2}\right) \right). \end{aligned} \tag{A3b}$$

For $b'c'$ ($-\infty < \zeta \leq 0$) the corresponding mapping is

$$W = \frac{q_s}{2\pi} \int_0^\zeta \frac{dt}{(t-1)\sqrt{t}} = \frac{iq_s}{2\pi} \int_\zeta^0 \frac{dt}{(1-t)\sqrt{-t}} = \frac{iq_s}{\pi} \tan^{-1} \sqrt{-\zeta}. \tag{A3c}$$

A2. Mapping of the Inverse Hodograph Plane

[14] Mapping of the dZ/dW plane onto the ζ plane results in

$$\frac{dZ}{dW} = C_3 \int_0^\zeta \frac{dt}{\sqrt{t(t-1)}} + C_4, \tag{A4a}$$

where C_3 and C_4 are constants. The branch of \sqrt{t} is selected which is positive at $t > 0$ while $\sqrt{t-1}$ is positive at $t > 1$. Using the values at point c' ($\zeta = 0$, $dZ/dW = -i/c$),

$$\frac{-i}{c} = C_4. \tag{A4b}$$

At point a' ($\zeta = 1$, $dZ/dW = -i/k$),

$$\begin{aligned} \frac{-i}{k} &= C_3 \int_0^1 \frac{dt}{\sqrt{t(t-1)}} - \frac{i}{c} = -iC_3 \int_0^1 \frac{dt}{\sqrt{t(1-t)}} - \frac{i}{c} \\ &= -iC_3\pi - \frac{i}{c}; \end{aligned} \tag{A4c}$$

therefore

$$C_3 = \frac{1}{\pi} \left(\frac{1}{k} - \frac{1}{c} \right). \tag{A4d}$$

Substituting the values of C_3 and C_4 in equation (A4a) gives equation (3). Along $c'f'a'$ ($0 \leq \zeta \leq 1$) the mapping of equation (3) becomes

$$\begin{aligned} \frac{dZ}{dW} &= \frac{-i}{\pi} \left(\frac{1}{k} - \frac{1}{c} \right) \int_0^\zeta \frac{dt}{\sqrt{t(1-t)}} - \frac{i}{c} \\ &= -i\frac{2}{\pi} \left(\frac{1}{k} - \frac{1}{c} \right) \sin^{-1} \sqrt{\zeta} - \frac{i}{c}. \end{aligned} \tag{A5a}$$

For the segment $d'b'$ ($1 \leq \zeta < \infty$) the dZ/dW mapping is

$$\begin{aligned} \frac{dZ}{dW} &= \frac{1}{\pi} \left(\frac{1}{k} - \frac{1}{c} \right) \left(\int_0^1 \frac{dt}{\sqrt{t(t-1)}} + \int_1^\zeta \frac{dt}{\sqrt{t(t-1)}} \right) - \frac{i}{c} \\ &= \frac{1}{\pi} \left(\frac{1}{k} - \frac{1}{c} \right) \int_1^\zeta \frac{dt}{\sqrt{t(t-1)}} - \frac{i}{k} \end{aligned} \tag{A5b}$$

so that

$$\frac{dZ}{dW} = \frac{2}{\pi} \left(\frac{1}{k} - \frac{1}{c} \right) \cosh^{-1} \sqrt{\zeta} - \frac{i}{k}. \tag{A5c}$$

Finally, the mapping for $c'b'$ ($-\infty < \zeta \leq 0$) can be obtained as

$$\begin{aligned} \frac{dZ}{dW} &= \frac{1}{\pi} \left(\frac{1}{k} - \frac{1}{c} \right) \int_0^\zeta \frac{dt}{\sqrt{-t(1-t)}} - \frac{i}{c} \\ &= \frac{2}{\pi} \left(\frac{1}{k} - \frac{1}{c} \right) \sinh^{-1} \sqrt{-\zeta} - \frac{i}{c}. \end{aligned} \tag{A5d}$$

A3. Mapping of the Physical Plane

[15] Since

$$\frac{dZ}{d\zeta} = \frac{dZ}{dW} \frac{dW}{d\zeta}, \tag{A6}$$

using equations (2) and (3),

$$\frac{dZ}{d\zeta} = \left(\frac{1}{\pi} \left(\frac{1}{k} - \frac{1}{c} \right) \int_0^\zeta \frac{dt}{\sqrt{t(t-1)}} - \frac{i}{c} \right) \frac{q_s}{2\pi(1-\zeta)\sqrt{\zeta}}. \tag{A7}$$

Integrating equation (A7),

$$Z = \int_0^\zeta \left(\frac{1}{\pi} \left(\frac{1}{k} - \frac{1}{c} \right) \int_0^t \frac{d\tau}{\sqrt{\tau(\tau-1)}} - \frac{i}{c} \right) \frac{q_s}{2\pi(1-t)\sqrt{t}} dt + C_5. \tag{A8a}$$

Using the point c' ($\zeta = 0$, $Z = -iy$), $C_5 = -iy$, so

$$Z = \int_0^\zeta \left(\frac{1}{\pi} \left(\frac{1}{k} - \frac{1}{c} \right) \int_0^t \frac{d\tau}{\sqrt{\tau(\tau-1)}} - \frac{i}{c} \right) \frac{q_s}{2\pi(1-t)\sqrt{t}} dt - iy, \tag{A8b}$$

which, after manipulation, gives equation (4). For $c'b'$ or $(-\infty < \zeta \leq 0)$,

$$c = \frac{q_s}{T} \tag{A10b}$$

$$Z = \frac{q_s}{2\pi^2} \left(\frac{1}{k} - \frac{1}{c} \right) \int_0^\zeta \left(\int_0^t \frac{d\tau}{\sqrt{-\tau(1-\tau)}} \right) \frac{dt}{(1-t)i\sqrt{-t}} - \frac{iq_s}{2\pi c} \int_0^\zeta \frac{dt}{(1-t)i\sqrt{-t}} - iy. \tag{A9a}$$

and

$$y = \frac{2q}{\pi^2} \left(\frac{1}{k} - \frac{1}{c} \right) 2G$$

Letting $-t = \tan^2 \theta$,

or

$$\int_0^\zeta \frac{dt}{(1-t)\sqrt{-t}} = -2 \tan^{-1} \sqrt{-\zeta} \tag{A9b} \qquad \left(\frac{1}{k} - \frac{1}{c} \right) = \frac{\pi^2}{4G} \frac{y}{q_s} \tag{A10c}$$

and letting $-\tau = \sinh^2 \theta$,

Solving Equations (A10b) and (A10c) simultaneously,

$$\int_0^t \frac{d\tau}{\sqrt{-\tau(1-\tau)}} = -2 \sinh^{-1} \sqrt{-t}, \tag{A9c} \qquad q_s = k \left(T + \frac{\pi^2}{4G} y \right) \tag{A10d}$$

so equation (A9a) converts to

$$c = \frac{k}{T} \left(T + \frac{\pi^2}{4G} y \right). \tag{A10e}$$

$$Z = \frac{q_s}{\pi c} \tan^{-1} \sqrt{-\zeta} - i \left(y - \frac{q_s}{2\pi^2} \left(\frac{1}{k} - \frac{1}{c} \right) \int_0^\zeta \frac{\sinh^{-1} \sqrt{-tdt}}{(1-t)\sqrt{-t}} \right). \tag{A9d}$$

A4. Position of the Phreatic Line

[16] The equation of phreatic line $d'b'$ ($1 \leq \zeta < \infty$) is given by

Furthermore, letting $-t = \sinh^2 \tau$,

$$Z = \int_\infty^\zeta \left(\frac{2}{\pi} \left(\frac{1}{k} - \frac{1}{c} \right) \cosh^{-1} \sqrt{t} - \frac{i}{k} \right) \frac{q_s}{2\pi(1-t)\sqrt{t}} dt + \frac{T}{2}, \tag{A11a}$$

$$\int_0^\zeta \frac{\sinh^{-1} \sqrt{-tdt}}{(1-t)\sqrt{-t}} = \int_0^{\sinh^{-1} \sqrt{-\zeta}} \frac{\tau d\tau}{\cosh \tau}, \tag{A9e}$$

which can be rewritten as

resulting in equation (5). In general,

$$Z = \frac{q_s}{\pi^2} \left(\frac{1}{k} - \frac{1}{c} \right) \int_\infty^\zeta \frac{\cosh^{-1} \sqrt{t}}{(1-t)\sqrt{t}} dt - \frac{iq_s}{2\pi k} \int_\infty^\zeta \frac{dt}{(1-t)\sqrt{t}} + \frac{T}{2}. \tag{A11b}$$

$$\int \frac{\tau d\tau}{\cosh \tau} = \frac{\tau^2}{2} - \frac{\tau^4}{8} + \frac{5\tau^6}{144} - \dots + \frac{(-1)^n E_n \tau^{2n+2}}{(2n+2)(2n)!} + \dots, \tag{A9f}$$

Letting $t = \cosh^2 \tau$, the first integral is

where $E_n = nth$ Euler number, while

$$\int_\infty^\zeta \frac{\cosh^{-1} \sqrt{t}}{(1-t)\sqrt{t}} dt = 2 \int_{\cosh^{-1} \sqrt{\zeta}}^\infty \frac{\tau d\tau}{\sinh \tau} \tag{A11c}$$

$$\int_0^\infty \frac{\tau d\tau}{\cosh \tau} = 2G. \tag{A9g}$$

and the second integral is

At point b' ($\zeta = -\infty, Z = T/2$),

$$\int_\infty^\zeta \frac{dt}{(1-t)\sqrt{t}} = -2 \ln \tanh \left(\frac{\cosh^{-1} \sqrt{\zeta}}{2} \right); \tag{A11d}$$

$$\frac{T}{2} = \frac{q_s}{\pi c} \tan^{-1} \infty - i \left(y - \frac{2q_s}{\pi^2} \left(\frac{1}{k} - \frac{1}{c} \right) \int_0^\infty \frac{\tau d\tau}{\cosh \tau} \right). \tag{A10a}$$

subsequently, equation (A11b) converts into

Equating real and imaginary parts,

$$Z = \frac{T}{2} + \frac{2q_s}{\pi^2} \left(\frac{1}{k} - \frac{1}{c} \right) \int_{\cosh^{-1} \sqrt{\zeta}}^\infty \frac{\tau d\tau}{\sinh \tau} + \frac{iq_s}{\pi k} \ln \tanh \left(\frac{\cosh^{-1} \sqrt{\zeta}}{2} \right). \tag{A11e}$$

$$T = \frac{q_s}{c}$$

Substituting values of q_s and c yields equation (9). At point a' ($\zeta = 1$) the phreatic line has a vertical asymptote given by equation (11) because

$$\int_0^{\infty} \frac{\tau d\tau}{\sinh \tau} = \frac{\pi^2}{4}, \quad (\text{A12a})$$

while

$$\int \frac{\tau d\tau}{\sinh \tau} = \tau - \frac{\tau^3}{18} + \frac{7\tau^5}{1800} - \dots + \frac{(-1)^n 2(2^{2n} - 1)B_n \tau^{2n+1}}{(2n+1)!} + \dots, \quad (\text{A12b})$$

where $B_n = n$ th Bernoulli number.

A5. Relationship for Channel Perimeter

[17] The shape of the perimeter of the channel is given by equation (5):

$$X + iY = \frac{T}{\pi} \tan^{-1} \sqrt{-\zeta} - i \left(y - \frac{y}{2G} \int_0^{\sinh^{-1} \sqrt{-\zeta}} \frac{\tau d\tau}{\cosh \tau} \right). \quad (\text{A13a})$$

Equating real and imaginary parts,

$$X = \frac{T}{\pi} \tan^{-1} \sqrt{-\zeta} \quad (\text{A13b})$$

$$Y = - \left(y - \frac{y}{2G} \int_0^{\sinh^{-1} \sqrt{-\zeta}} \frac{\tau d\tau}{\cosh \tau} \right). \quad (\text{A13c})$$

Equations (A13b) and (A13c) are parametric equations for the shape of the channel perimeter. From equation (A13b),

$$\sqrt{-\zeta} = \tan \left(\frac{\pi X}{T} \right). \quad (\text{A13d})$$

Plugging ζ into equation (A13c) yields equation (8).

A6. Variation in Seepage Velocity

[18] The distribution of the velocity of seeping water normal to the channel perimeter can be found by substituting the value of c in equation (13) and manipulating

$$\frac{u + iv}{u^2 + v^2} = \frac{\pi}{2G} \frac{y}{q_s} \sinh^{-1} \sqrt{-\zeta} - \frac{iT}{q_s}. \quad (\text{A14a})$$

Eliminating q_s and separating real and imaginary parts,

$$\frac{u}{u^2 + v^2} = \frac{\pi}{2Gk(T + \pi^2 y/4G)} \sinh^{-1} \sqrt{-\zeta} \quad (\text{A14b})$$

$$\frac{v}{u^2 + v^2} = - \frac{T}{k(T + \pi^2 y/4G)}. \quad (\text{A14c})$$

Squaring and adding these equations,

$$\frac{u^2 + v^2}{(u^2 + v^2)^2} = \frac{1}{V^2} = \left(\frac{\pi}{2Gk(T/y + \pi^2/4G)} \right)^2 + \left(\frac{T/y}{k(T/y + \pi^2/4G)} \right)^2, \quad (\text{A14d})$$

which gives

$$V = \frac{k(T/y + \pi^2/4G)}{\sqrt{((\pi \sinh^{-1} \sqrt{-\zeta})/2G)^2 + (T/y)^2}}. \quad (\text{A14e})$$

Equation (A13d) can be used to eliminate ζ in equation (A14e) to get equation (14).

[19] **Acknowledgments.** The All India Council for Technical Education, New Delhi, has sponsored this study under the scheme Career Award for Young Teachers (1-15/FD/CA(18)/2001-2002). Their financial support is duly acknowledged. The author would like to thank A. R. Kacimov and two other anonymous reviewers for their insightful review and constructive suggestions, which resulted in a significant improvement of the manuscript.

References

- Anakhaev, K. N. (2004), Free percolation and seepage flows from water-courses, *J. Fluid Dyn.*, 39(5), 756–761.
- Aravin, V. I., and S. N. Numerov (1965), *Theory of Flow in Undeformable Porous Media*, Isr. Program for Sci. Transl., Jerusalem.
- Chahar, B. R. (2000), Optimal design of channel sections considering seepage and evaporation losses, Ph.D. thesis, Univ. of Roorkee, Roorkee, India.
- Chahar, B. R. (2001), Extension of Vederikov's graph for seepage from canals, *Ground Water*, 39(2), 272–275.
- Chahar, B. R. (2005), Seepage from canals, project report, All India Council for Tech. Educ., New Delhi.
- Chow, V. T. (1973), *Open Channel Hydraulics*, McGraw-Hill, New York.
- Harr, M. E. (1962), *Groundwater and Seepage*, McGraw-Hill, New York.
- Hunt, B. W. (1972), Seepage from shallow open channel, *J. Hydraul. Div. Am. Soc. Civ. Eng.*, 98(HY5), 779–785.
- Huyakorn, P. S., and G. F. Pinder (1983), *Computational Methods in Subsurface Flow*, Elsevier, New York.
- Ilyinskii, N. B., and A. R. Kacimov (1984), Seepage limitation optimization of the shape of an irrigation channel by the inverse boundary value problem method, *J. Fluid Dyn.*, 19(4), 404–410.
- Kacimov, A. R. (2001), Optimal shape of a variable condenser, *Proc. R. Soc. London, Ser. A*, 457, 485–494.
- Kacimov, A. R. (2003), Discussion of "Design of minimum seepage loss nonpolygon canal sections" by Prabhata K. Swamee and Deepak Kashyap, *J. Irrig. Drain. Eng.*, 129(1), 68–70.
- Kacimov, A. R., and Y. V. Obnosov (2002), Analytical determination of seeping soil slopes of a constant exit gradient, *Z. Angew. Math. Mech.*, 82(6), 363–376.
- Kovacs, G. (1981), *Seepage Hydraulics*, Elsevier, New York.
- Liggett, J. A., and P. L.-F. Liu (1983), *The Boundary Integral Equation Method for Porous Media Flow*, Allen and Unwin, St. Leonards, N. S. W., Australia.
- Morel-Seytoux, H. J. (1964), Domain variations in channel seepage flow, *J. Hydraul. Div. Am. Soc. Civ. Eng.*, 90(HY2), 55–79.
- Muskat, M. (1982), *Flow of Homogeneous Fluids Through Porous Media*, Int. Hum. Resour. Dev. Corp., Boston.
- Polubarinova-Kochina, P. Y. (1962), *Theory of Groundwater Movement*, Princeton Univ. Press, Princeton, N. J.
- Remson, I., G. M. Hornberger, and F. J. Molz (1971), *Numerical Methods in Subsurface Hydrology*, Wiley-Interscience, Hoboken, N. J.
- Strack, O. D. L. (1989), *Groundwater Mechanics*, Prentice-Hall, Upper Saddle River, N. J.

- Strack, O. D. L., and M. I. Asgian (1978), A new function for use in the hodograph method, *Water Resour. Res.*, 14, 1045–1058.
- Swamee, P. K., and D. Kashyap (2001), Design of minimum seepage loss nonpolygon canal sections, *J. Irrig. Drain. Eng.*, 127(2), 113–117.
- Swamee, P. K., G. C. Mishra, and B. R. Chahar (2000), Design of minimum seepage loss canal sections, *J. Irrig. Drain. Eng.*, 126(1), 28–32.
- Swamee, P. K., G. C. Mishra, and B. R. Chahar (2001a), Closure to discussion of “Design of minimum seepage loss canal sections,” *J. Irrig. Drain. Eng.*, 127(3), 191–192.
- Swamee, P. K., G. C. Mishra, and B. R. Chahar (2001b), Design of minimum seepage loss canal sections with drainage layer at shallow depth, *J. Irrig. Drain. Eng.*, 127(5), 287–294.

B. R. Chahar, Department of Civil Engineering, Indian Institute of Technology Delhi, Hauz Khas, New Delhi 110 016, India. (chahar@civil.iitd.ac.in)